International Journal of Energy Production and Management
https://www.acadlore.com/journals/IJEPM

Enhancement of Solar Distillation Efficiency Using Mesh Cotton Fabric: A Case Study in Kirkuk City-Iraq

Sahip Z. Akbara[1,2*], Naseer T. Alwan[3]

[1] Technical Engineering College, Northern Technical University, 36001 Kirkuk, Iraq
[2] Renewable Energy Research Center, Northern Technical University, 36001 Kirkuk, Iraq
[3] College of Oil & Gas Techniques Engineering, Northern Technical University, 36001 Kirkuk, Iraq

* Correspondence: Sahip Z. Akbara (sahip.zainalabdeen24gs@ntu.edu.iq)

Received: 10-02-2025 **Revised:** 11-15-2025 **Accepted:** 12-12-2025

Citation: S. Z. Akbara and N. T. Alwan, "Enhancement of solar distillation efficiency using mesh cotton fabric: A case study in Kirkuk city-Iraq," *Int. J. Energy Prod. Manag.*, vol. 10, no. 4, pp. 730–743, 2025. https://doi.org/10.56578/ijepm100412.

Abstract: Given the extreme scarcity of water in arid regions, innovative solutions are essential to provide potable water. Among these solutions, solar desalination technology stands out, using sunlight to evaporate saltwater and then condense it to convert it into fresh water. However, conventional solar desalination systems face challenges related to production efficiency, which is affected by factors such as solar radiation intensity, wind speed, and temperature. This research aims to improve the efficiency of these systems using mesh cotton. Studies have shown that mesh cotton absorbs more sunlight, increasing the evaporation rate, while wood acts as a thermal insulator and enhances the system's efficiency. The experiment revealed a 37% increase in water production from the improved distillate. The conventional system produced 1,300 ml of distilled water per day, while the improved system produced 1,742 ml per day. These improvements indicate that the use of readily available materials can significantly improve the efficiency of solar desalination systems, helping address water scarcity in arid regions.

Keywords: Solar energy; Solar still; Low-cost materials; Thermal efficiency; Climate adaptation

1 Introduction

Water scarcity is a major global issue that is increasingly exacerbated by climate change affecting most parts of the world. While freshwater resources are abundant in urban areas, rural and remote areas face significant challenges in accessing potable water. Water pollution rates have also increased significantly due to industrial development, making clean water difficult to obtain in some areas. In this context, the use of solar distillation technologies is an effective and suitable solution. Solar distillation systems are an affordable and viable option, particularly in regions with abundant solar energy providing clean, potable water in rural and remote areas is one of the most significant challenges facing developing countries, with industrial pollution exacerbating this problem. For example, a recent study in the Indian state of Kerala showed that the Periyar River is suffering from a severe decline in water quality due to the discharge of 17.35 million liters of toxic industrial waste daily, including heavy metals and pesticides, making the water unfit for irrigation or human use. Globally, UN reports indicate that about 10% of the world's population, or approximately 720 million people, live in countries experiencing high and critical levels of water stress, which particularly affects rural areas [1–3]. Access to fresh water is one of the most significant challenges facing communities in remote and arid areas. Recent reports show that more than 2.2 billion people around the world lack access to safe drinking water services, and four out of five people who lack basic water services live in rural areas [4]. Improving access to safe drinking water in rural areas has significantly increased life expectancy. The health benefits became more evident five years after the water supply improvements, as these improvements were associated with reduced rates of water-related diseases, thus easing pressure on healthcare systems [5]. According to a World Health Organization report, approximately 2.1 billion people worldwide still lack access to safe drinking water. The majority of these individuals live in remote and rural communities where freshwater supply systems face significant challenges [6]. Freshwater constitutes only about 2.5% of the total water on Earth, while saltwater (such as seawater and ocean water) constitutes about 97.5% of this small percentage of freshwater, less than 1% is in the form of surface water available for direct human use, making available freshwater sources extremely limited [7]. The salinity of

seawater ranges between 35,000 and 45,000 parts per million (ppm), making it unfit for direct human consumption. According to the World Health Organization, drinking water should contain less than 500 ppm of total dissolved solids (TDS) to ensure its quality and safety for human consumption [8]. Due to the scarcity of available freshwater, many countries rely on desalination technologies as their primary source of drinking water. Technologies such as reverse osmosis (RO) and multi-stage distillation (MSF) are used to convert salty seawater into fresh, drinkable water [9]. However, large amounts of fossil fuels are consumed in the production process. Studies have shown that approximately 130 million tons of oil are consumed annually to produce 13 million cubic meters of drinking water per day [10]. Fossil fuels reportedly account for approximately 78.3% of the world's primary energy source, while renewable energy and nuclear energy account for 19.2% and 2.5%, respectively, according to data released in 2016 [11, 12]. For the above reasons, numerous studies have been conducted on the use of renewable and clean energy sources, such as solar energy, which is a sustainable and environmentally friendly option in many different applications [13, 14]. Researchers have used renewable energy to convert saltwater or seawater into potable or fresh water, particularly in remote areas where fresh water sources are difficult to obtain [15]. Therefore, solar stills can be considered an optimal alternative due to their low cost and low maintenance requirements [16]. This method is used to remove germs and other contaminants from water, leaving it clean and potable. Solar still production is significantly affected by both weather conditions and the design of the device [17]. While solar stills offer many advantages, they also have some drawbacks. Their production is not as abundant as other technologies. As a result, significant efforts have been made to improve device design and the selection of materials used in solar stills to increase their effectiveness and production efficiency [18]. Solar stills have been the focus of numerous studies aimed at improving their efficiency and evaporation and condensation mechanisms. Previous studies have explored various methods to enhance the performance of solar stills using different fabric-based materials. Ahmed et al. [19] demonstrated that incorporating cotton material in a cylindrical solar still improved productivity and efficiency by 29.11% and 24.45%, respectively, while reducing production cost by 40.21%. Similarly, Alwan et al. [20] reported that the use of black cloth yielded the most significant improvement, increasing distilled water productivity by approximately 20% compared to other materials under identical conditions. In contrast, Abbaspour et al. [21] investigated the influence of wick materials in a vertical solar still and found that black cotton outperformed gauze, resulting in a 5.1% increase in productivity. Wiener et al. [22] examined a fabric coated with polyurethane rollers featuring capillary properties and achieved an energy efficiency of 62.16% with a daily yield of 1.14 $\mathrm{L/m^2}$. Furthermore, Agrawal et al. [23] studied the use of black jute fabric and observed a 62% enhancement in cumulative productivity compared to a conventional still. Collectively, these studies indicate that fabric-based modifications particularly those using black or absorbent materials can significantly enhance thermal absorption and water evaporation rates. Studies have shown that black cotton mesh has a superior ability to absorb solar radiation compared to other materials. The black color enhances the absorption of sunlight and converts it into heat, raising the temperature of the water inside the still and thus accelerating the evaporation process. Furthermore, the black cotton mesh reduces heat loss due to convection with the surrounding air, improving the overall thermal efficiency of the system. The fabric mesh structure also helps distribute heat evenly across the surface of the water inside the still, promoting balanced evaporation and increasing the overall efficiency of the system. However, most prior work focused on solid or woven fabrics, while the effect of mesh cotton, especially black cotton mesh, remains underexplored. Therefore, the present study aims to address this gap by experimentally investigating the influence of black cotton mesh on the performance of solar stills under local climatic conditions.

2 Experimental Setup

Figure 1 illustrates the design of the solar still used in this study, which involves two single-slope solar panels in Kirkuk, Iraq (latitude: $35.4686°$, longitude: $44.38933°$). To optimize solar radiation absorption, the panels were oriented southward, with an area of 1 square meter per panel. Given Kirkuk's geographical location, the glass covers of the stills were tilted at a $35°$, corresponding to the latitude. 1 cm thick Russian wood was used to construct the structure. To ensure the system's efficiency and reduce energy losses, a silicone rubber strip was applied around the edges of the clamps to prevent vapor leakage.

The wooden structure was painted matte black, including the interior surfaces of the basins, to further enhance heat absorption. Furthermore, a black mesh fabric (50 cm long and 1 m wide) was installed within the system to increase solar radiation absorption and enhance evaporation, details in Table 1. This fabric was selected based on its high solar absorption capacity. To reduce heat loss, glass wool insulation was used around the edges of the system, contributing to reduced thermal leakage. A channel was designed within the distiller to improve water flow, while maintaining the water level in the basin at approximately 1 cm to ensure optimal evaporation conditions. The experimental trials were conducted from July 25 to 27, 2025, in the extremely hot environment of Kirkuk. Figure 2 presents conventional and modified solar still systems, both featuring similar structural configurations, such as transparent glass covers for solar transmission and wooden support bases. The figure also shows the experimental setup, including the positioning of the solar panels, the placement of the black mesh fabric, and the applied insulation,

offering a realistic view of the system used in this study. Notably, the modified still incorporates design enhancements aimed at improving heat retention and evaporation, thereby increasing freshwater production.

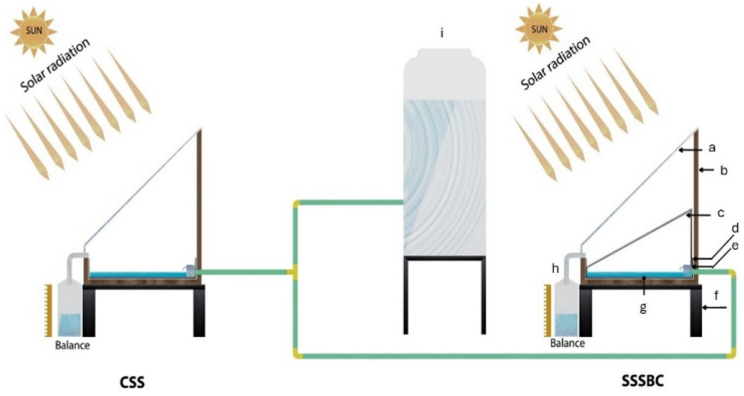

Figure 1. Schematic diagram of the suggested solar still (SSSBC), and conventional solar still (CSS): a. Transparent Plexiglass cover, b. MDF, c. Cotton cloth, d. The water basin, e. Mechanical floater, f. Metal legs, g. The basin water, h. Graduated cylinder, i. Feed water tank

Figure 2. The conventional solar still (left) and the modified solar still (right) used to evaluate performance improvements in freshwater production under identical environmental conditions

Table 1. The dimensions and structural of the solar still

Tools Used	Value
Solar still area	1 m^2
Glass tilt angle	35°
Glass thickness	4 mm
Glass wool insulation thickness	1 cm
Black paint	Matte
Black cloth buckle	Matte cotton
Wood fish	1 cm
Waterproofing material	Thermal silicon
Water basin length	98 cm
Water basin width	48 cm

2.1 Modified Model

In the proposed solar still system, mesh cotton is a crucial component in improving the thermal efficiency of the device. In this research, a solar distillation system was modified by using a mesh cotton, which contributes to improving the system's thermal efficiency, the details of the suggested solar still (SSSBC) illustrated in Table 2. The mesh cotton enhances the absorption of solar radiation, accelerating the evaporation process, as demonstrated by Zarda et al. [24] and Tei et al. [25] both focused on enhancing the performance of solar thermal systems but approached the problem from different perspectives. Zarda et al. [24] analyzed the thermal performance of a flat plate

solar collector (FPSC) using diamond/water nanofluids at various concentrations, numerically simulating the system under the hot climate of Iraq with ANSYS/FLUENT. Their results showed that a 1% nanofluid concentration yielded the highest thermal efficiency of 68.90%, representing a 12.2% improvement over pure water due to enhanced thermal conductivity and improved heat transfer. In contrast, Tei et al. investigated a modified solar still incorporating a black rubber mat as a low-cost thermal storage material. Experimental results revealed that the modification increased total water yield from 1.99 kg to 2.82 kg and improved thermal efficiency from 34.90% to 54.80%, along with a notable 1.16% rise in exergy efficiency. While Zarda et al. [24] emphasized numerical modeling and nanoparticle-based heat transfer enhancement to boost collector efficiency, Tei et al. [25] demonstrated a practical, low-cost material solution to improve potable water production and system efficiency.

Table 2. Specifications of system

Ingredients	Specifications	Dimensions / Materials
Steaming basin	Made of black-painted Russian wood for increased heat absorption	Area: 1 square meter, thickness: 1 cm of Russian wood
The solar distillation device flew	The structural frame is made of Russian wood for increased durability	Area: 1 square meter, thickness: 1 cm of Russian wood
Glass cover	4 mm thick clear glass	Inclined at an angle of 35°
Black cloth	To improve the absorption of solar radiation	Length: 50 cm , width: 1 m
Isolation	Glass wool to reduce heat loss	It is mounted around the edges of the solar distiller
Water channel	Water flow control system to maintain the water level	Water level: 1 cm in the aquarium
Silicone	To prevent steam leakage around the edges of the glass cover	It is applied around the edges of the glass cover

Figure 3. Mesh cotton inside the improved solar distiller

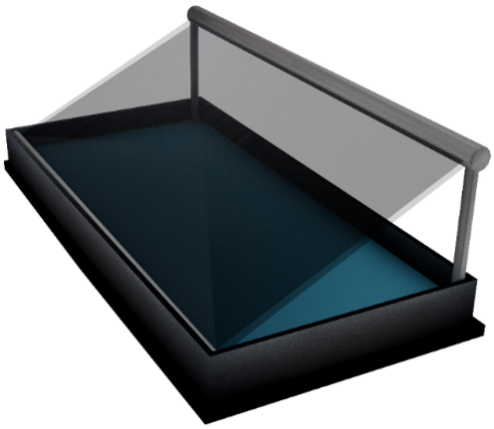

Figure 4. Three-dimensional view of the solar still basin showing the slanted transparent glass cover and the black-colored basin liner used for effective solar energy absorption and water evaporation

Thanks to its high capacity to absorb solar radiation and convert it into heat, the black mesh cotton contributes to raising the water temperature inside the tank and effectively increasing the evaporation rate. It also reduces heat loss through conduction to the surrounding air, improving heat retention within the system. Black mesh fabric was used

in the proposed system, as shown in the Figure 3 and Figure 4, which illustrates the fabric's installation and fixation method.

The TDS and salinity were measured using a handheld digital TDS meter with an accuracy of ±2%. Measurements were taken at the outlet collection point during peak operating hours. The TDS values of the distilled water were found to be in the range of 5–15 mg/L, which is considerably lower than the World Health Organization (WHO) drinking-water guideline limit of 500 mg/L, confirming its suitability for potable use. Correspondingly, the measured salinity levels ranged from 0.01–0.05 ppt, indicating an effective removal of dissolved impurities.

2.2 Method of Experimentation

The experimental setup for the solar stills was designed to provide optimal conditions for evaluating the performance of both systems. To maximize sunlight absorption, the stills were oriented southward, and the glass covers were sealed with silicone rubber to prevent vapor leakage. The water tanks were maintained at a constant water level of approximately 1 cm using a regulated conduit system. During the experiment, measurements were taken hourly from 8:00 a.m. to 6:00 p.m. A K-type data logger was used to record various temperature readings, including: (i) the temperature at the bottom of the solar still water tank (Tw_1), (ii) the temperature at the water surface (Tw_2), (iii) the temperature inside the Plexiglas cover (Tg_1), and (iv) the temperature outside the plastic cover (Tg_2). In addition, a mercury thermometer was used to measure the ambient air temperature, while a TM solar meter recorded the hourly solar radiation intensity. Figure 5 illustrates the experimental setup of the solar still system, which harnesses solar radiation to purify or desalinate water through the natural processes of evaporation and condensation. Solar energy passes through a transparent glass cover and is absorbed by a black-colored basin liner (a) that holds a shallow layer of saline or impure water (b). The black surface enhances heat absorption, raising the water temperature and promoting evaporation. The resulting water vapor rises and condenses upon contact with the cooler inner surface of the glass cover (c), forming water droplets. These droplets flow down the inclined glass into a distillate channel (d), which collects the condensed fresh water and directs it into a container (i) placed on a balance to measure the distilled water yield. To monitor the system's performance, several instruments are connected to a data logger (e). A thermocouple (g) measures the temperature at different points, such as the basin water, glass surface, and ambient air. A pyranometer (h) records the intensity of solar radiation, while an anemometer (f) measures wind speed, which affects the cooling rate of the condensation surface. All these readings are continuously logged and analyzed to assess the thermal efficiency and productivity of the solar still system.

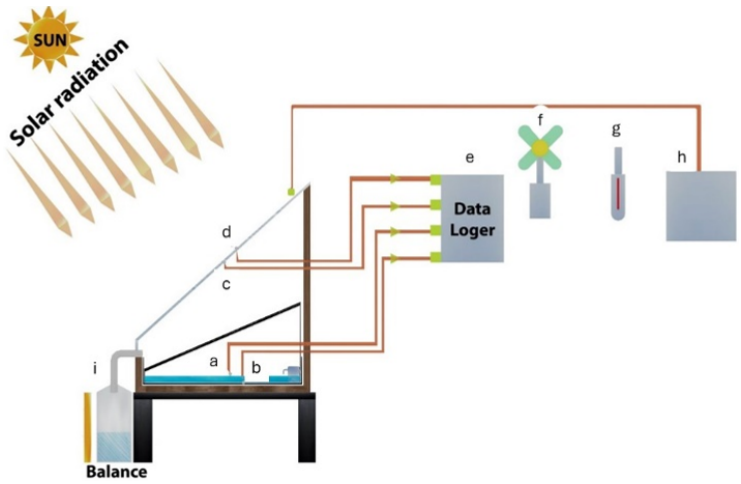

Figure 5. Schematic diagram of the experimental setup for a solar still system, illustrating the process of water desalination and purification through solar radiation, evaporation, and condensation

2.3 Energy Balance and Uncertainty Propagation

This uncertainty analysis is an essential step to give the experimental findings more dependability. The accuracy values for each measurement instrument utilized in the research must be ascertained before beginning the uncertainty analysis [26, 27]. The accuracy values and measurement range for every measuring device are shown in Table 2. The uncertainty analysis was then conducted using the equations below:

$$\mathrm{Standarddeviation(S)} = \sqrt{\frac{\sum_{\mathrm{i}=1}^{\mathrm{n}} \left(\mathrm{xi} - \mathrm{x}'\right)^2}{\mathrm{n} - 1}} \tag{1}$$

$$\text{Standarderror(S.E)} = \frac{\text{s}}{\sqrt{\text{n}}} \tag{2}$$

$$\text{Error }\% \frac{\text{S.E}}{\text{X}'} \times 100 \tag{3}$$

$$\text{X}' = \frac{\sum_{\text{i=1}}^{\text{n}} \text{Xi}}{\text{n}} \tag{4}$$

The measured value (Xi), the meaning of the measured values (X'), and the number of measurements (n) are all inputs into the formula.

$$\eta_{\text{ss-th}} = \frac{\text{m}_{\text{ew}} \times \text{h}_{\text{fg}}}{\text{i}_{\text{(t)s}} \times \text{A}_{\text{s}}} \tag{5}$$

The average latent heat (h_{fg}) in Eq. (6) [18]:

$$\text{h}_{\text{fg}} = 10^3 \left[2501.9 - 2.40706 \times \text{T}_{\text{w}} + 1.192217 \times 10^{-3} \times \text{T}_{\text{bw}}^2 - 1.5863 \times 10^{-5} \times \text{T}_{\text{w}}^3\right] \tag{6}$$

$$\text{m}_{\text{ew}} = \frac{\text{h}_{\text{ev}} \left(\text{T}_{\text{w}} - \text{T}_{\text{g}}\right) \text{A}_{\text{s}}}{\text{h}_{\text{fg}}} \tag{7}$$

In the experiments, distilled water was recorded as the collected volume V over each hourly interval. The volume was converted to mass musing the water density at the measured water temperature ρ_t; for the temperatures in our range, the small density variation was accounted for when calculating $\dot{\text{m}} = \frac{\text{m}}{\Delta \text{t}} = \frac{\rho \text{V}}{\Delta \text{t}}$.

To motivate the above efficiency formula and to identify major loss terms, a simple energy balance is written for the still control volume over Δt.

$$\text{Q}_{\text{in}} = \text{Q}_{\text{evap}} + \text{Q}_{\text{cond}} + \text{Q}_{\text{conv}} + \text{Q}_{\text{rad}} + \Delta \text{Q}_{\text{storage}} \tag{8}$$

Experimental uncertainties in measured quantities (m/V of collected water, temperatures used to compute h_{fg}, solar irradiance I, and area A) propagate into the estimated efficiency. Using first-order (linearized) propagation, the standard uncertainty in η, denoted σ_η, follows:

$$\sigma_\eta = \sqrt{\left(\frac{\partial \eta}{\partial \text{m}} \sigma_{\text{m}}\right)^2 + \left(\frac{\partial \eta}{\partial \text{T}} \sigma_{\text{T}}\right)^2 + \left(\frac{\partial \eta}{\partial \text{I}} \sigma_{\text{I}}\right)^2 + \left(\frac{\partial \eta}{\partial \text{A}} \sigma_{\text{A}}\right)^2} \tag{9}$$

$$\frac{\partial \eta}{\partial \text{m}} = \frac{\text{h}_{\text{fg.avg}}}{\text{IA}\Delta \text{t}} \tag{10}$$

$$\frac{\partial \eta}{\partial \text{T}} = \frac{\text{m}}{\text{IA}\Delta \text{t}} \frac{\text{h}_{\text{fg}}}{\Delta \text{T}} \tag{11}$$

$$\frac{\partial \eta}{\partial \text{I}} = -\frac{\text{m}\, \text{h}_{\text{fg.avg}}}{\text{I}^2 \text{A}\Delta \text{t}} \tag{12}$$

$$\frac{\partial \eta}{\partial \text{A}} = -\frac{\text{m}\, \text{h}_{\text{fg.avg}}}{\text{IA}^2 \Delta \text{t}} \tag{13}$$

In these expressions $\frac{\text{dh}_{\text{fg}}}{\text{dT}}$ is obtained analytically from Eq. (6) (for the linear relation above $\frac{\text{dh}_{\text{fg}}}{\text{dT}} = -2.361 \times 10^3$ J.kg^{-1}.°C^{-1}). Use the instrument accuracy and precision reported in Table 3 to estimate $\sigma_{\text{m}}, \sigma_{\text{T}}, \sigma_{\text{I}}$. For example: σ_{I} may be taken as the solar meter percent error (2% of measured I), σ_{T} from the thermocouple/data-logger uncertainty (1.9 °C in Table 2), and σ_{m} from the volumetric measurement procedure (graduated cylinder resolution and repeatability; convert volume uncertainty to mass through ρ_t). If multiple repeated measurements are available, use the standard deviation of repeated mass measurements as σ_{m}. Finally σ_{A} is typically negligible if area is known precisely; if not, include the manufacturing tolerance.

Putting these together gives a quantitative σ_η for each hourly interval. Reporting $\eta \pm \sigma_\eta$(or 95% CI using $1.96\,\sigma_\eta$) gives readers a clear sense of confidence in the measured efficiency improvement (e.g., the reported 37% increase in yield between SSSBC and conventional solar still (CSS) should be accompanied by uncertainty bounds computed from the above).

Table 3. Accuracy, measurement error, and operating range for each device

Equipment	The Accuracy	Measuring Range	Error Range%	The Unit
Anemometer	82%	0–25	1.8	$\mathrm{m/s}$
Data logger	98%	-200–1370	1.9	°C
TM- solar power meter	98%	0–2000	2	$\mathrm{W/m^2}$
Thermocouple	98%	-100–200	1.9	°C

3 Results and Discussion

This research compares the efficiency of two distinct solar still designs: one that uses no active components at all (a passive solar still) and another that incorporates a mesh cotton for enhanced performance (an upgraded solar still). A more efficient still is possible with the addition of black mesh cloth, which increases the still's capacity to absorb solar radiation, convert it to heat more efficiently, hasten evaporation, and ultimately increase water production. The design also helps retain water heat for longer, improving overall system efficiency. Important design considerations include material quality and installation techniques, as well as environmental conditions such as solar radiation intensity and temperature, which affect the daily output of solar stills. Thanks to these improvements, the improved black mesh fabric is still more efficient than a passive still at producing distilled water, making it an excellent choice for solar-powered desalination projects.

3.1 The Effect of Weather Conditions

The study showed the influence of the main environmental factors on the performance of the solar distillation device, since a clear contrast in temperature and intensity of solar radiation was observed during the test day. Temperatures started at $39.6°$ at 8 a.m. to reach a peak of $71.8°$ at 1 p.m., while solar radiation peaked at noon at $1002\ \mathrm{W/m^2}$ on the surface of the distillery. The data also recorded a gradual decrease for both indicators as sunset approaches, as Figure 6 shows the temporal changes of these parameters during a day (July 27, 2025) in Kirkuk.

Solar stills' performance was clearly affected by temperature and the strength of the sun's rays over the whole trial. From 3 in the morning until 1 in the afternoon, temperatures rose steadily, reaching a top of 71.8 degrees Celsius. At midday, the sun's rays reached their strongest point, at 1,002 watts per square meter. In light of these findings, it is clear that environmental factors significantly affect solar still. An increase in the intensity of the sun's rays causes the water inside the still to boil, which speeds up the evaporation process and increases the amount of water that can be distilled. To maximize water production efficiency, it is crucial to optimize the device's exposure to sunlight.

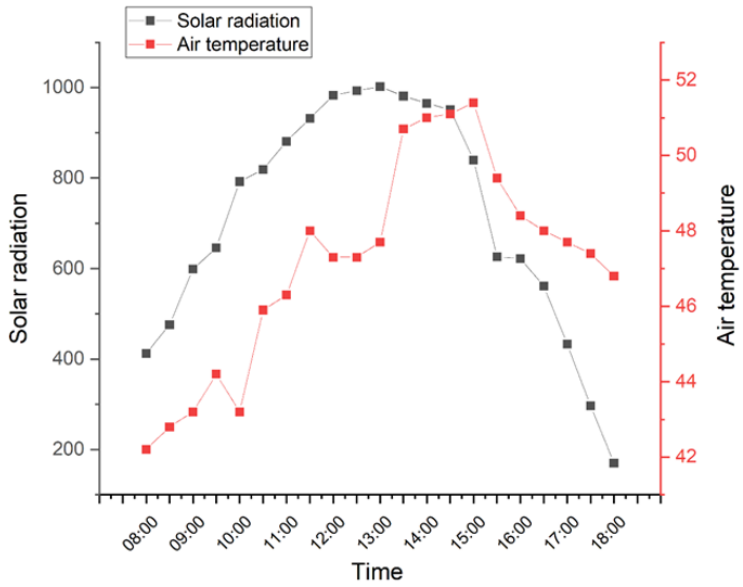

Figure 6. Daily fluctuations in ambient temperatures and solar energy levels

To maximize the effectiveness of solar stills, factors like relative humidity and wind speed are crucial. These external variables have an immediate effect on the cooling of the glass cover, which speeds up the condensation of vapor and boosts the system's overall efficiency. On July 27, 2025, the temperature and relative humidity changed

with time, as seen in Figure 7. The correlation between these factors and the device's effectiveness is evident in the data collected over the course of 11 hours.

According to the findings, solar still efficiency is very sensitive to variations in wind speed and relative humidity. Condensation efficiency and productivity were affected by changes in these parameters, which caused oscillations in the temperature differential between the water surface and the glass cover. The findings show that controlling the relative humidity and wind speed is the key to making standard and enhanced solar stills work better in the real world.

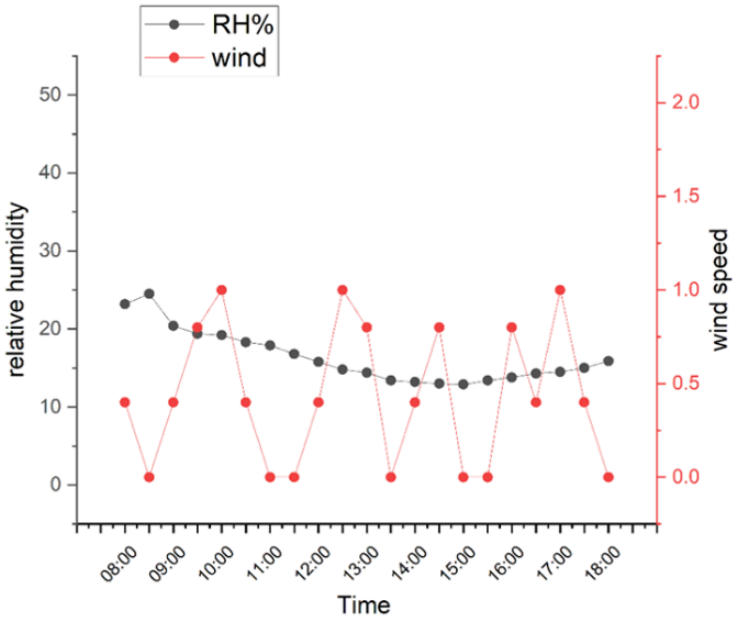

Figure 7. Fluctuations in wind speed and relative humidity around the clock

The performance of a solar still can be improved by using a black mesh fabric. This fabric absorbs solar radiation more efficiently, raising the temperature of the water inside the tank. As shown in Figure 8, the temperature for the SSSBC condition is generally higher than for the CSS condition, indicating a variation in temperature between the two conditions during the course of the day. The chart suggests that the SSSBC condition results in consistently higher temperatures compared to the CSS condition, though both follow a similar pattern over time. This fabric helps raise the temperature of the water inside the system, which in turn raises the temperature inside the still by reducing heat loss and enhancing heat retention.

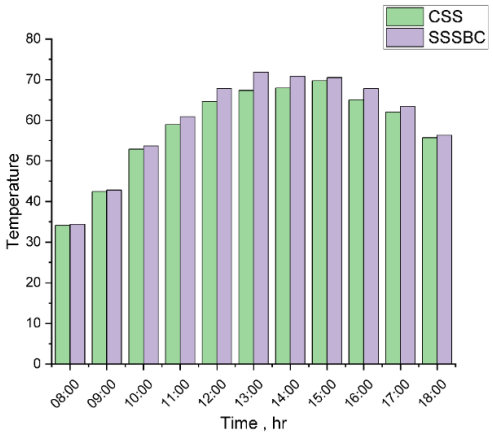

Figure 8. Water temperature changes over the clock for suggested solar still (SSSBC) and conventional solar still (CSS) systems

Furthermore Figure 9 presents a distillation process saw a 37% increase in the output of the active solar still, producing 1,742 ml of distilled water compared to 1,265 ml for the passive still. The black mesh fabric absorbs more sunlight, improving heat retention and increasing the evaporation rate, which increases the yield. As a result, the

temperature in the active still continues to rise. The active still produced 1,742 ml on July 27, 2025, which was 37% more than the passive still's 1,300 ml.

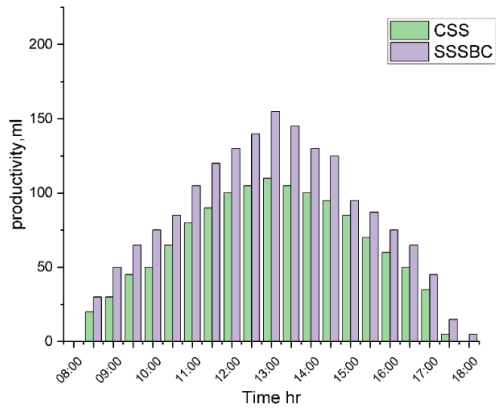

Figure 9. Comparison of productivity across different times of the day, from 08:00 to 18:00, for two conditions: suggested solar still (SSSBC) and conventional solar still (CSS)

Analyzing the performance of active or passive solar distillation systems relies heavily on evaluating thermal efficiency. According to the studies [28–30], a unique assessment is carried out in this regard to gauge the thermal efficiency of passive solar distillers as shown in Figure 10. The chart presents that the SSSBC consistently demonstrates higher thermal efficiency than the conventional solar still throughout the day. The efficiency of both systems increases from morning to midday, reaching peak values around 13:00 to 14:00. However, the SSSBC achieves significantly greater efficiency at all time intervals, indicating that the proposed design offers improved thermal performance compared to the conventional model.

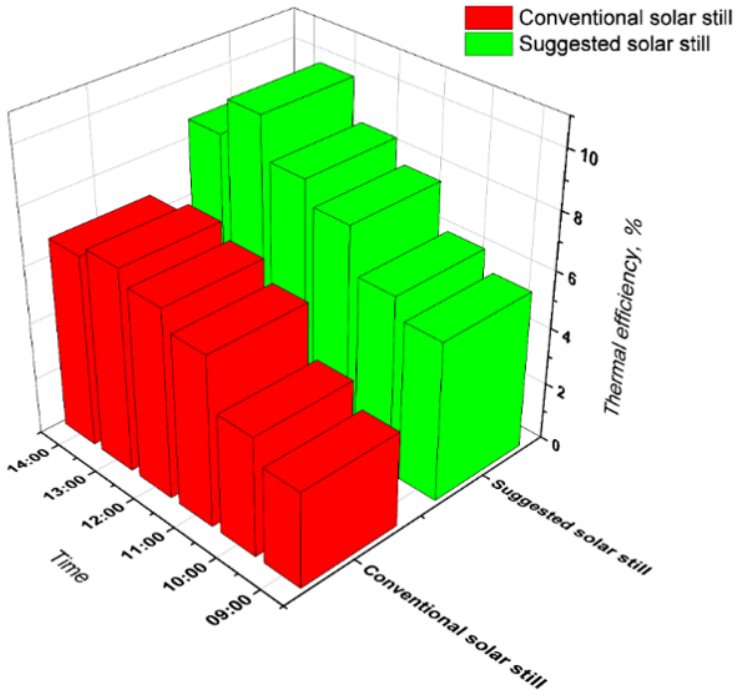

Figure 10. 3D bar chart comparing the thermal efficiency of a conventional solar still (CSS) and a suggested solar still (SSSBC) at different times of the day (09:00-14:00) for a typical day, July 27, 2025

3.2 Analysis of Production Cost

Aside from the obvious objective of increasing daily desalinated water output utilising solar energy, production costs also need to be considered. The key elements determining the yearly cost of generating one litre of desalinated water were examined in depth in certain study by Alwan et al. [18] using economic analysis. Among these parameters

are the following: capital cost (CS), depreciation fund factor (SFF), first annual cost (FAC), annual scrap value (ASV), annual cost (AC), annual maintenance cost (AMC), and yearly cost per litre (YCPL). calculated as follows:

$$\mathrm{CRF} = \frac{\mathrm{i}(1+\mathrm{i})^{\mathrm{n}}}{[\mathrm{i}(1+\mathrm{i})^{\mathrm{n}} - 1]} \tag{14}$$

$$\mathrm{SFF} = \frac{\mathrm{i}}{[\mathrm{i}(1+\mathrm{i})^{\mathrm{n}} - 1]} \tag{15}$$

$$\mathrm{FAC} = \mathrm{SC} \times \mathrm{CRF} \tag{16}$$

According to Shehata et al. [31] the salvage value of solar water desalination was 0.2 times the CS of manufacture and installation. Hence, the following is the formula for determining the ASV:

$$\mathrm{ASV} = \mathrm{S} \times \mathrm{SFF} \tag{17}$$

Fifteen percent of the initial yearly cost is AMC. According to Kabeel et al. [32] the annual cost was thus determined in this way:

$$\mathrm{AC} = \mathrm{FAC} + \mathrm{AMC} - \mathrm{ASV} \tag{18}$$

Finally, the yearly cost per liter (YCPL) as follows:

$$\mathrm{YCPL} = \frac{\mathrm{AC}}{\mathrm{SAP}} \tag{19}$$

The economic analysis employed a service life (depreciation) of n = 10 years for both the conventional and modified stills, which reflected the expected useful life of the low-cost construction materials (MDF/wood, plexiglass, seals) and is consistent with similar small-scale solar-still studies. A nominal annual interest rate of i = 12% was used to compute CRF and SFF. The 12% rate was chosen as a conservative representative of prevailing commercial lending/discount rates and local inflation conditions relevant to the study period (2024–2025) and aligns with the financial assumptions commonly used in comparative analyses of small renewable-energy systems (see Shehata et al. [31] and Kabeel et al. [32] for related practice). Under these choices the capital-recovery and sinking-fund factors were calculated using Eqs. (14) and (15). Table Table 4 summarizes the manufacturing and installation costs of the CSS and the SSSBC. Both systems use similar materials, but the SSSBC includes additional cotton components to enhance performance. The total cost is $84 for the CSS and $109 for the SSSBC, indicating a slightly higher expense for the modified design due to the added materials.

Table 4. Manufacturing and installation capital cost (CS) of solar stills, $

Type Material	Quality	CSS ($)	SSSBC ($)
Wooden board with a thickness of 1.8 cm	2 m^2	30	30
Plexiglass cover with a thickness of 0.3 cm	1.2 m^2	10	10
Silicone glue	2 pieces	3	3
Aluminum waterway	2 pieces	5	5
Aluminum basin	1 piece	15	15
Solar still base	1 piece	10	10
Thermal insulation glass wool	2 pieces	5	5
Heat resistant black paint	2 pieces	4	4
Cotton cloth	1 m		5
cotton fabric structure			20
Mechanical water float	1 piece	1	1
The total cost		84	109

Which match the numerical factors reported in Table 5. Additional economic assumptions were: (i) salvage value S = 0.2CS (20% of capital cost) as adopted from Shehata et al. [31]; (ii) annual maintenance cost assumed as 15% of the first annual cost (AMC = 0.15·FAC) following Kabeel et al. [32]; (iii) all costs were expressed in USD at local market prices collected during 2025; and (iv) taxes, subsidies, and financing fees were excluded so that the analysis represents a pre-tax, straight-line economic comparison. These assumptions and their sources were used consistently to compute FAC, ASV, AMC, AC and, finally, YCPL reported in Table 5.

Table 5. Unit costs analysis for water produced in dollars

The Item	CSS	SSSBC
Solar still life expectancy, n	10	10
Interest rate per year, i	12	12
Capital cost (CS), $	84	109
The factor for the recovery of capital (CRF)	0.1769	0.1769
The factor for the sinking fund (SFF)	0.0569	0.0569
The first annual (yearly) cost (FAC), $	14.505	18.043
The worth of salvage (S), $	16.4	20.4
The value of annual salvation (ASV), $	0.933	1.16
The cost of annual maintenance (AMC), $	2.175	2.706
annual (yearly) cost (AC), $	15.748	19.589
Yearly yield from the solar still system	474.5	635.83
Yearly cost per liter(YCPL), $	0.0349	0.0329

3.3 Results from Solar Distillation Compared: A Black Fabric Affects Output

Previous research has investigated solar distillation systems that employed black cloth or other enhancement methods to improve productivity. To evaluate the effectiveness of the current design, its performance was compared with those studies. Table 6 presents this comparison, showing that the productivity improvement achieved in the present study is comparable to the results of previous experimental works, with differences primarily attributed to variations in climatic conditions and design parameters.

Table 6. Comparison of solar distillation results

The Study	Productivity Rate	Maximum Solar Radiation Intensity (W/m^2)	Location	Research Aspect
Current study	37%	1102 W/m^2	Iraq	Experimental
Tei et al. [25]	54%	1050 W/m^2	India	Experimental
Hassan [33]	37%	1100 W/m^2	Egypt	Experimental
Dumka et al. [34]	33%	1150 W/m^2	Romania	Experimental
Aghakhani et al. [35]	44%	1075 W/m^2	Iran	Experimental

4 Conclusions

This study demonstrates that integrating black mesh cotton into a single-slope solar still significantly enhances freshwater productivity under the climatic conditions of Kirkuk, Iraq. The modified configuration achieved a daily distillate yield of 1,742 mL compared with 1,300 mL for the conventional design, corresponding to an approximate 37% performance increase. The enhancement is attributed to the fabric's strong solar absorptivity, which promoted higher water temperatures, reduced thermal losses, and improved evaporation–condensation dynamics. The system also benefited from wooden structural insulation, which minimized heat dissipation.

Furthermore, water quality assessment confirmed that the distillate satisfied WHO potable water limits in terms of salinity and TDS, supporting its suitability for drinking applications. Economic analysis revealed that the yearly cost per liter of desalinated water decreased marginally in the modified still compared with the conventional system, affirming its feasibility as a low-cost solution for decentralized freshwater production.

Limitations and Future Perspectives

Although the improved system demonstrated promising water productivity, several limitations should be acknowledged. First, the results were obtained during a short measurement period in summer, and therefore do not capture seasonal variations in weather conditions. Second, the performance was evaluated under a single water depth and fixed mesh configuration; different fabric geometries, colors, and orientations may further influence heat transfer and yield. The study also employed passive heat enhancement only, without integrating advanced thermal storage, forced circulation, or hybridization approaches, which could substantially increase efficiency. Lastly, durability and degradation of the cotton mesh under long-term exposure were not assessed, leaving uncertainties regarding lifespan and maintenance frequency.

Recommendations for Future Work

Future studies should investigate year-round system performance under varying climatic conditions and explore alternative wick or absorber materials with improved durability and heat absorption. Modified geometries or hybrid configurations with thermal storage or solar collectors could further raise distillate yield. Incorporating automated

water-level and performance monitoring may enhance operational efficiency, while long-term material degradation and cost assessments are needed to support large-scale deployment in remote regions.

Data Availability

The data used to support the research findings are available from the corresponding author upon request.

Conflicts of Interest

The authors declare no conflicts of interest.

References

[1] S. Senevirathna, S. Ramzan, and J. Morgan, "A sustainable and fully automated process to treat stored rainwater to meet drinking water quality guidelines," *Process Saf. Environ. Prot.*, vol. 130, pp. 190–196, 2019. https://doi.org/10.1016/j.psep.2019.08.005

[2] B. Mohamad, "Improving heat transfer performance of flat plate water solar collectors using nanofluids," *J. Harbin Inst. Technol.*, vol. 32, no. 2, pp. 80–89, 2025. https://doi.org/10.11916/j.issn.1005-9113.2024001

[3] H. H. M. Ali, A. M. Hussein, K. M. H. Allami, and B. Mohamad, "Evaluation of shell and tube heat exchanger performance by using ZnO/water nanofluids," *J. Harbin Inst. Technol.*, vol. 30, no. 6, pp. 62–69, 2023. https://doi.org/10.11916/j.issn.1005-9113.2023001

[4] M. Salehi, "Global water shortage and potable water safety; today's concern and tomorrow's crisis," *Environ. Int.*, vol. 158, p. 106936, 2022. https://doi.org/10.1016/j.envint.2021.106936

[5] X. Shen, M. A. R. Sarkar, Z. Liang, and T. Zhang, "Health impact of rural drinking water safety program in China: Implications for life span of rural residents," *Environ. Sustain. Indic.*, vol. 27, p. 100874, 2025. https://doi.org/10.1016/j.indic.2025.100874

[6] F. F. Qader, F. Z. Mohammed, and B. Mohamad, "Thermodynamic analysis and optimization of flat plate solar collector using TiO2/water nanofluid," *J. Harbin Inst. Technol.*, 2023. https://doi.org/10.11916/j.issn.1005-9113.2023050

[7] F. F. Qader, B. Mohamad, A. M. Hussein, and S. H. Danook, "Numerical study of heat transfer in circular pipe filled with porous medium," *Pollack Periodica*, vol. 19, no. 1, pp. 137–142, 2023. https://doi.org/10.1556/606.2023.00869

[8] O. E. Olufisayo and O. Olanrewaju, "A review of renewable energy powered seawater desalination treatment process for zero waste," *Water*, vol. 16, no. 19, p. 2804, 2024. https://doi.org/10.3390/w16192804

[9] R. Miri, B. Mliki, B. A. Mohamad, M. A. Abbassi, M. Oreijah, K. Guedri, and S. Abderafi, "Entropy generation and heat transfer rate for MHD forced convection of nanoliquid in presence of viscous dissipation term," *CFD Lett.*, vol. 15, no. 12, pp. 77–106, 2023. https://doi.org/10.37934/cfdl.15.12.77106

[10] F. Muhammad-Sukki, A. B. Munir, R. Ramirez-Iniguez, S. H. Abu-Bakar, S. H. Mohd Yasin, S. G. McMeekin, and B. G. Stewart, "Solar photovoltaic in Malaysia: The way forward," *Renew. Sustain. Energy Rev.*, vol. 16, no. 7, pp. 5232–5244, 2012. https://doi.org/10.1016/j.rser.2012.05.002

[11] E. B. Agyekum, F. Amjad, L. Shah, and V. I. Velkin, "Optimizing photovoltaic power plant site selection using analytical hierarchy process and density-based clustering—Policy implications for transmission network expansion, Ghana," *Sustain. Energy Technol. Assess.*, vol. 47, p. 101521, 2021. https://doi.org/10.1016/j.seta.2021.101521

[12] F. Amjad, E. B. Agyekum, L. A. Shah, and A. Abbas, "Site location and allocation decision for onshore wind farms, using spatial multi-criteria analysis and density-based clustering: A techno-economic-environmental assessment, Ghana," *Sustain. Energy Technol. Assess.*, vol. 47, p. 101503, 2021. https://doi.org/10.1016/j.seta.2021.101503

[13] S. J. Yaqoob, A. L. Saleh, S. Motahhir, E. B. Agyekum, A. Nayyar, and B. Qureshi, "Comparative study with practical validation of photovoltaic monocrystalline module for single and double diode models," *Sci. Rep.*, vol. 11, no. 1, p. 19153, 2021. https://doi.org/10.1038/s41598-021-98593-6

[14] E. B. Agyekum, "Techno-economic comparative analysis of solar photovoltaic power systems with and without storage systems in three different climatic regions, Ghana," *Sustain. Energy Technol. Assess.*, vol. 43, p. 100906, 2021. https://doi.org/10.1016/j.seta.2020.100906

[15] F. M. Abed and D. S. Mahmood, "Experimental study of the effect for water depth on the mass transfer of passive solar still chemical solutions," *Tikrit J. Eng. Sci.*, vol. 24, no. 2, pp. 1–10, 2022. https://doi.org/10.25130/tjes.24.2.01

[16] T. Rajaseenivasan, T. Elango, and K. K. Murugavel, "Comparative study of double basin and single basin solar stills," *Desalination*, vol. 309, pp. 27–31, 2013. https://doi.org/10.1016/j.desal.2012.09.014

[17] H. G. Hameed, "Experimentally evaluating the performance of single slope solar still with glass cover cooling and square cross-section hollow fins," *Case Stud. Therm. Eng.*, vol. 40, p. 102547, 2022. https://doi.org/10.1016/j.csite.2022.102547

[18] N. T. Alwan, S. E. Shcheklein, and O. M. Ali, "Experimental study and economic cost analysis about enhancement productivity for a conventional solar still combined with humidifiers ultrasonic," *Energy Sources, Part A: Recovery, Utilization, Environ. Eff.*, vol. 47, no. 1, pp. 7802–7818, 2021. https://doi.org/10.1080/15567036.2021.1924318

[19] M. M. Z. Ahmed, F. Alshammari, U. F. Alqsair, M. Alhadri, A. S. Abdullah, and M. Elashmawy, "Experimental study on the effect of the black wick on tubular solar still performance," *Case Stud. Therm. Eng.*, vol. 38, p. 102333, 2022. https://doi.org/10.1016/j.csite.2022.102333

[20] N. T. Alwan, B. M. Ali, O. R. Alomar, N. M. Abdulrazzaq, O. M. Ali, and R. M. Abed, "Performance of solar still units and enhancement techniques: A review investigation," *Heliyon*, vol. 10, no. 18, p. e37693, 2024. https://doi.org/10.1016/j.heliyon.2024.e37693

[21] M. Abbaspour, Q. Esmaili, and A. Ramiar, "Improving vertical solar still performance for efficient desalination: Investigating the influence of wick, condensate plate and device dimensions," *Solar Energy*, vol. 272, p. 112468, 2024. https://doi.org/10.1016/j.solener.2024.112468

[22] J. Wiener, M. Z. Khan, and K. Shah, "Performance enhancement of the solar still using textiles and polyurethane rollers," *Sci. Rep.*, vol. 14, no. 1, p. 5202, 2024. https://doi.org/10.1038/s41598-024-55948-z

[23] A. Agrawal, R. S. Rana, and P. K. Srivastava, "Application of jute cloth (natural fibre) to enhance the distillate output in solar distillation system," *Mater. Today: Proc.*, vol. 5, no. 2, pp. 4893–4902, 2018. https://doi.org/10.1016/j.matpr.2017.12.066

[24] F. Zarda, A. Hussein, S. Danook, and B. Mohamad, "Enhancement of thermal efficiency of nanofluid flows in a flat solar collector using CFD," *Diagnostyka*, vol. 23, no. 4, pp. 1–9, 2022. https://doi.org/10.29354/diag/156384

[25] E. A. Tei, R. Mohideen, S. Noman, and et al., "Performance improvement of solar still by water mass splitting arrangement," *Sci. Rep.*, vol. 15, p. 30965, 2025. https://doi.org/10.1038/s41598-025-15849-1

[26] N. T. Alwan, S. E. Shcheklein, and O. M. Ali, "Productivity of enhanced solar still under various environmental conditions in Yekaterinburg city/Russia," *IOP Conf. Ser.: Mater. Sci. Eng.*, vol. 791, p. 012052, 2020. https://doi.org/10.1088/1757-899X/791/1/012052

[27] N. T. Alwan, S. E. Shcheklein, and O. M. Ali, "A practical study of a rectangular basin solar distillation with single slope using paraffin wax (PCM) cells," *Int. J. Energy Convers.*, vol. 7, no. 4, pp. 162–170, 2019. https://doi.org/10.15866/irecon.v7i4.17862

[28] K. Sampathkumar, T. V. Arjunan, and P. Senthilkumar, "The experimental investigation of a solar still coupled with an evacuated tube collector," *Energy Sources, Part A: Recovery Util. Environ. Eff.*, vol. 35, no. 3, pp. 261–270, 2013. https://doi.org/10.1080/15567036.2010.511426

[29] A. A. Hachicha and E. M. Abo-Zahhad, "Dust effect on solar energy systems and mitigation methods," *Int. J. Energy Prod. Manag.*, vol. 8, no. 2, pp. 97–105, 2023. https://doi.org/10.18280/ijepm.080206

[30] A. Agarwal, M. Ilunga, K. Tempa, and B. K. Humagai, "CFD analysis of solar air heater using V-shaped artificial roughness to attain heat transfer enhancement," *Int. J. Energy Prod. Manag.*, vol. 9, no. 3, pp. 171–180, 2024. https://doi.org/10.18280/ijepm.090306

[31] A. I. Shehata, A. E. Kabeel, M. M. K. Dawood, A. M. Elharidi, A. Abd-Elsalam, K. Ramzy, and A. Mehanna, "Enhancement of the productivity for single solar still with ultrasonic humidifier combined with evacuated solar collector: An experimental study," *Energy Convers. Manag.*, vol. 208, p. 112592, 2020. https://doi.org/10.1016/j.enconman.2020.112592

[32] A. E. Kabeel, A. M. Hamed, and S. A. El-Agouz, "Cost analysis of different solar still configurations," *Energy*, vol. 35, no. 7, pp. 2901–2908, 2010. https://doi.org/10.1016/j.energy.2010.03.021

[33] H. Hassan, "Comparing the performance of passive and active solar stills incorporating parabolic trough collector," *Renew. Energy*, vol. 148, pp. 437–450, 2020. https://doi.org/10.1016/j.renene.2019.10.050

[34] P. Dumka, A. Jain, and D. R. Mishra, "Energy, exergy, and economic analysis of single slope conventional solar still augmented with ultrasonic fogger," *Energy Storage*, vol. 30, p. 101541, 2020. https://doi.org/10.1016/j.est.2020.101541

[35] S. Aghakhani, A. Hajatzadeh Pordanjani, and M. Afrand, "Enhancing the performance of solar stills using porous materials and vibration: An experimental comparison of classic, wire mesh, and vibrating wire," *Energy Convers. Manag.*, vol. 344, p. 120250, 2025. https://doi.org/10.1016/j.enconman.2025.120250

Nomenclature

CSS	suggested solar still
SSSBC	suggested solar still
S	standard deviation
m_{ew}	the yearly yield from the solar still system, Kg/m^2
$m^{\cdot}$	mass collection rate of distilled water, kgs^{-1}
Δt	time interval
A	aperture area of the still m^2
A_w	exposure area, m^2
V	volume of distilled water, mL
T_W	surface temperature
T_∞	ambient temperature
Tg	glass-cover temperature
L	solar radiation intensity, l/m^2day
$I_{(t)}$	solar radiation intensity, W/m^2
CRF	factor for the sinking fund
SFF	the factor for the sinking fund
SAP	the solar still system's annual production
FAC	the first annual(yearly) cost, $
CS	the manufacturing and installation capital cost, $
ASV	value of annual salvation, $
AC	annual (yearly) cost, $
AMC	cost of annual maintenance, $
YCPL	the yearly cost-per-liter

Greek symbols

η	thermal effeciency
ρ_t	density at measured temperature, kg.m^{-3}

Subscripts

h_{fg}	average latent heat of vaporization, J/kg
h_{ev}	latent heat of evaporation, J/kg
hc	convective heat transfer coefficient
σ_m	the volumetric measurement procedure
σ_T	the thermocouple/data-logger uncertainty
σ_I	the solar meter percent error
σ_A	the standard deviation of repeated mass measurements
$\circ$	degree angle